Immunity
Article

Human Effector and Memory CD8+ T Cell Responses to Smallpox and Yellow Fever Vaccines

Joseph D. Miller,[1,2] Robbert G. van der Most,[1,2] Rama S. Akondy,[1] John T. Glidewell,[1] Sophia Albott,[1] David Masopust,[1] Kaja Murali-Krishna,[1] Patryce L. Mahar,[1] Srilatha Edupuganti,[1] Susan Lalor,[1] Stephanie Germon,[1] Carlos Del Rio,[1] Mark J. Mulligan,[1] Silvija I. Staprans,[1,3] John D. Altman,[1] Mark B. Feinberg,[1,3] and Rafi Ahmed[1,*]
[1]Emory Vaccine Center and the Hope Clinic, Emory University School of Medicine, Atlanta, GA 30322, USA
[2]These authors contributed equally to this work.
[3]Present Address: Merck Vaccines and Infectious Diseases, Merck and Company, West Point, PA 19486, USA.
*Correspondence: ra@microbio.emory.edu
DOI 10.1016/j.immuni.2008.02.020

SUMMARY

To explore the human T cell response to acute viral infection, we performed a longitudinal analysis of CD8+ T cells responding to the live yellow fever virus and smallpox vaccines—two highly successful human vaccines. Our results show that both vaccines generated a brisk primary effector CD8+ T cell response of substantial magnitude that could be readily quantitated with a simple set of four phenotypic markers. Secondly, the vaccine-induced T cell response was highly specific with minimal bystander effects. Thirdly, virus-specific CD8+ T cells passed through an obligate effector phase, contracted more than 90% and gradually differentiated into long-lived memory cells. Finally, these memory cells were highly functional and underwent a memory differentiation program distinct from that described for human CD8+ T cells specific for persistent viruses. These results provide a benchmark for CD8+ T cell responses induced by two of the most effective vaccines ever developed.

INTRODUCTION

Our understanding of primary antiviral CD8+ T cell responses to acute viral infections is largely based on experimental studies in mice. For example, infection of mice with lymphocytic choriomeningitis virus (LCMV) or vaccinia virus (VV) induces massive CD8+ T cell activation and expansion, such that 30%–80% of all splenic CD8+ T cells are virus-specific at 8 days after infection (Butz and Bevan, 1998; Harrington et al., 2002; Lukacher et al., 1999; Murali-Krishna et al., 1998). At the peak of the response, effector CD8+ T cells exhibit an activated phenotype, proliferate, produce interferon γ (IFN-γ) in response to antigen, and are highly susceptible to apoptosis (Butz and Bevan, 1998; Grayson et al., 2000; Lukacher et al., 1999; Murali-Krishna et al., 1998). The virus-specific CD8+ T cell pool contracts after viral clearance, with the remaining cells differentiating into long-lived memory T cells (Murali-Krishna et al., 1998). Long-term maintenance of these cells is antigen independent (Crotty et al., 2003; Demkowicz et al., 1996; Hammarlund et al., 2003; Lau et al., 1994; Murali-Krishna et al., 1999) and relies on interleukin 7 (IL-7)- and IL-15-driven homeostatic proliferation (Becker et al., 2002; Ku et al., 2000; Schluns et al., 2000; Tan et al., 2002; Wherry et al., 2002). In contrast, chronic infection dramatically changes the differentiation pathways of virus-specific CD8+ T cells, often resulting in altered T cell immunodominance, phenotype, migration, and function (Barber et al., 2006; Fuller and Zajac, 2003; van der Most et al., 2003; Wherry et al., 2004; Wherry et al., 2003a; Zajac et al., 1998).

To date, human antiviral CD8+ T cell responses have been extensively analyzed in the context of chronic infections, such as human immunodeficiency virus (HIV), cytomegalovirus (CMV), hepatitis C virus (HCV), and Epstein-Barr virus (EBV) (Barouch and Letvin, 2001; Callan et al., 1998; Hamann et al., 1997; Lauer et al., 2002; Lechner et al., 2000; McMichael and Rowland-Jones, 2001; Roos et al., 2000; Tan et al., 1999; Urbani et al., 2002; van Leeuwen et al., 2002). Such responses can be very robust, as exemplified by the massive clonal expansion of antigen-specific CD8+ T cells in acute infectious mononucleosis (Callan et al., 1998; Roos et al., 2000; Tan et al., 1999). Based on these studies, it has also become clear that the resulting populations of human CD8+ T cells display striking phenotypic differences, as determined by the expression profiles of surface markers like CD45RA, CD45RO, CD27, CD28, CCR7, and CD62L (Appay et al., 2002; Champagne et al., 2001; Sallusto et al., 1999; Tomiyama et al., 2004; van Leeuwen et al., 2002). For example, effector and central memory CD8+ T cells were defined on the basis of CD45RA and CCR7 expression patterns (Sallusto et al., 1999), leading to the following proposed differentiation scheme: $CD45RA^+CCR7^+$ (naive) → $CD45RA^-$ $CCR7^+$ (central memory T cells [T_{CM}]) → $CD45RA^-$ $CCR7^-$ (effector memory T cells [T_{EM}]) → $CD45RA^+CCR7^-$ ($CD45RA^+$ effector memory T cells [T_{EMRA}]) (Champagne et al., 2001). This differentiation scheme is complicated by the observation that different phenotypic subsets of CD8+ T cells accumulate in different chronic infections (Appay et al., 2002). For instance, terminally differentiated $CD45RA^+CCR7^-$ CD8+ T cells dominate the response in persistent CMV infection (Appay et al., 2002; Roos et al., 2000; van Leeuwen et al., 2002), whereas memory responses in HIV-infected individuals are dominated by intermediate effector memory cells ($CD45RA^-$ $CD27^+CD28^-CCR7^-$) (Appay et al., 2002). Altogether, these studies imply that viral persistence, whether chronic or latent, has a distinct impact on the differentiation pathways of antiviral CD8+ T cells.

The complex relationship between viral persistence and T cell differentiation (Appay et al., 2002) stresses the need for longitudinal analyses of antiviral T cell responses after acute viral infection in humans. Live-attenuated viral vaccines provide a potential model for acute viral infections. Two of the most effective vaccines known to medicine, the smallpox vaccine (Dryvax) and the yellow fever virus (YFV)-17D vaccine are live viruses that result in acute infections. Indeed, immunization with either vaccine results in viral replication and long-term protective immunity (Demkowicz and Ennis, 1993; Demkowicz et al., 1996; Littaua et al., 1992; McCarthy et al., 1958; Moss, 1999). The YFV-17D vaccine strain was isolated after consecutive passages in primary chicken embryo fibroblasts. Immunization results in a self-limiting viral infection and long-lived neutralizing antibody titers, i.e., neutralizing antibodies can persist for up to 30–35 years after vaccination (Poland et al., 1981). However, crucial parameters, such as the kinetics, magnitude, and specificity of the T cell response, remain largely unknown (Reinhardt et al., 1998), despite recently mapped HLA-B35 restricted epitopes (Co et al., 2002). The Dryvax smallpox vaccine contains live vaccinia virus (VV) isolated from the lymph of calves infected with the New York City Board of Health strain of VV (Wyeth, 2002). Neutralizing antibodies are detected in the blood at approximately 10 days after Dryvax immunization (McCarthy et al., 1958). VV-specific $CD4^+$ and $CD8^+$ effector T cells can be identified by antigen-stimulation assays at frequencies ranging from 0.1 to 1.1% of $CD4^+$ T cells and 0.4 to 3.7% of $CD8^+$ T cells at 2 weeks after primary vaccination (Amara et al., 2004). Consistent with their effector function, these cells express perforin and granzyme B (Rock et al., 2005). After the peak of the response, a long-lived pool of memory $CD8^+$ T cells is formed (Demkowicz et al., 1996) that expresses the IL-7 receptor (CD127) (Rock et al., 2006) and slowly diminishes over several decades (Crotty et al., 2003; Hammarlund et al., 2003).

Both vaccines offer the unique opportunity to investigate primary antiviral T cell responses after acute viral infection in the absence of antigenic re-exposure. Yellow fever virus is no longer endemic in the United States, and immunization with YFV-17D is now limited to visitors to high-risk areas and is not included in childhood vaccination programs in the Unites States. Similarly, the last reported case of smallpox occurred in 1978, and there is no known reservoir for the virus. Furthermore, with the exception of laboratory and some healthcare workers and military personnel, smallpox vaccination in the United States was discontinued in 1972.

In the present study, we used both these vaccines as models of acute viral infection in humans. We show that antiviral $CD8^+$ T cell responses occur rapidly, peaking around 2 weeks after immunization. At the peak of the response, up to 12.5% and 40% of peripheral $CD8^+$ T cells displayed an activated phenotype ($CD38^+$, HLA-DR $^+$, Ki-67 $^+$, Bcl-2^{low}) after immunization with YF-Vax and Dryvax, respectively, with no detectable evidence of bystander activation. Phenotypic analysis of VV-specific $CD8^+$ T cells revealed that all effector T cells expressed perforin and granzyme B at the peak of the response. The contraction and memory phase of the response was associated with further differentiation of VV-specific T cells. Altogether, our data support a model of human $CD8^+$ T cell differentiation in which naive $CD8^+$ T cells undergo massive expansion in response to antigen and pass through an effector phase prior to gradually differentiating into long-lived memory cells.

RESULTS

Identifying YF-Vax- and Dryvax-Induced Effector $CD8^+$ T Cells by Phenotypic Analysis

To test the notion that the human $CD8^+$ T cell response to acute viral infection would be associated with an emerging population of activated effector cells, we analyzed the expression patterns of a large set of surface and intracellular markers on $CD8^+$ T cells after immunization with the live-attenuated YFV (YF-Vax) or Dryvax smallpox vaccine. Although many markers displayed changed expression patterns after immunization, we found that only a small subset of phenotypic markers (CD38, HLA-DR, Ki-67, and Bcl-2) had sufficiently low preimmunization background expression to allow the unequivocal identification of the expanding populations of activated $CD8^+$ T cells. The emergence of a phenotypically discrete pool of effector T cells was subsequently confirmed by functional analyses and major histocompatibility complex (MHC) class I tetramer staining (see below).

HLA-DR and CD38 are well-described differentiation markers that are expressed by activated T cells during the acute phase of chronic and persistent viral infections in humans (Appay et al., 2002; Callan et al., 1998; Lechner et al., 2000). Analyzing the HLA-DR and CD38 expression patterns on peripheral $CD3^+$ $CD8^+$ peripheral blood mononuclear cells (PBMCs) at multiple time points after immunization allowed us to evaluate the magnitude and kinetics of the T cell responses after immunization. In both the YF-Vax and Dryvax immunization trials, we observed baseline expression of 0.5%–2% of $CD38^+$ HLA-DR^+ $CD8^+$ T cells in the PBMCs prior to vaccination (Figure 1A). After YF-Vax immunization, a substantial expansion of activated $CD38^+$ HLA-DR^+ $CD8^+$ T cells was detected in all vaccine recipients. This response was associated with a transient viremia. Viral RNA was detected in plasma at days 3 and 7 after immunization, peaking at day 7 (Figure 1A). The peak of the $CD8^+$ T cell response was observed at day 15 after immunization, when 4%–13% of peripheral $CD8^+$ T cells coexpressed CD38 and HLA-DR (Figure 1A). This percentage declined sharply in all volunteers by day 30 after immunization and remained at background levels during the memory phase of the T cell response. Even greater expansions of activated $CD8^+$ T cells were observed after Dryvax immunization (Figure 1B). At the peak of the response (day 14), 10%–40% of peripheral $CD8^+$ T cells expressed an activated phenotype. Similar to the YF-Vax-induced response, numbers of activated $CD8^+$ T cell declined after day 15, returning to baseline by day 30 after immunization.

To further characterize the effector T cell response induced by immunization, we measured expression of the proliferation marker Ki-67 (Gerdes et al., 1984) and the antiapoptotic protein Bcl-2 (Hockenbery et al., 1990) in $CD8^+$ T cells. Resting T cells do not express Ki-67, whereas cycling or recently divided T cells upregulate Ki-67 expression (Chakrabarti et al., 2000; Gerdes et al., 1984; Pitcher et al., 2002). Bcl-2 is a useful marker because its downregulation indicates susceptibility to apoptosis (Appay et al., 2002; Grayson et al., 2000). Indeed, over 99% of peripheral $CD8^+$ T cells exhibited a resting Ki-67^- Bcl-2^{high} phenotype before immunization, with less than 0.5% of $CD8^+$ T cells displaying

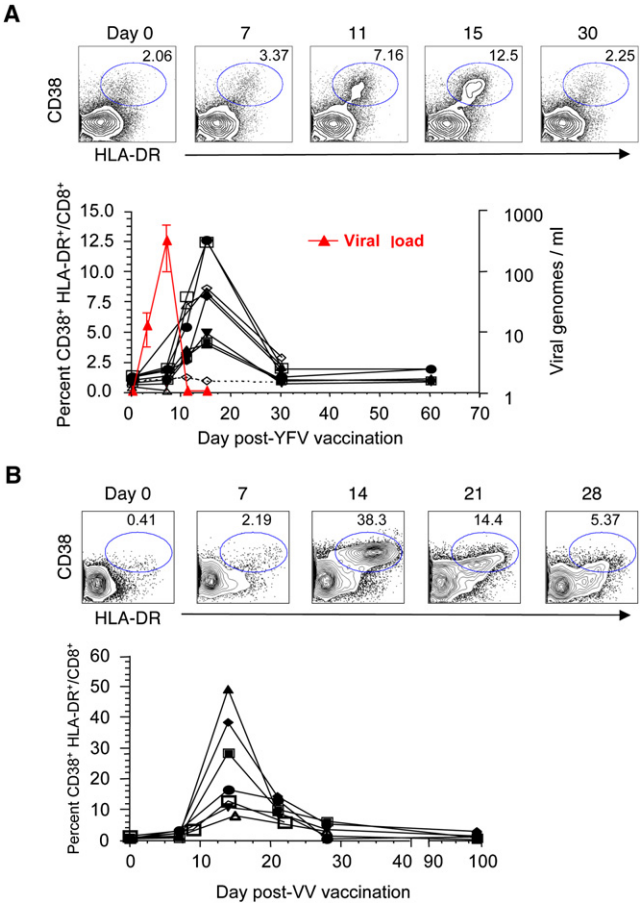

Figure 1. Identification of Activated CD8+ T Cells after Vaccination
CD38 and HLA-DR expression on CD8+ T cells after YF-Vax (A) or Dryvax (B) immunization. Heparinized whole-blood samples from vaccine recipients were stained with antibodies against CD3, CD8, CD38, and HLA-DR. FACS contour plots were gated on CD3+, CD8+ cells. YFV in the blood was quantitated by a real-time PCR. Error bars represent the standard error of the mean for three volunteers.

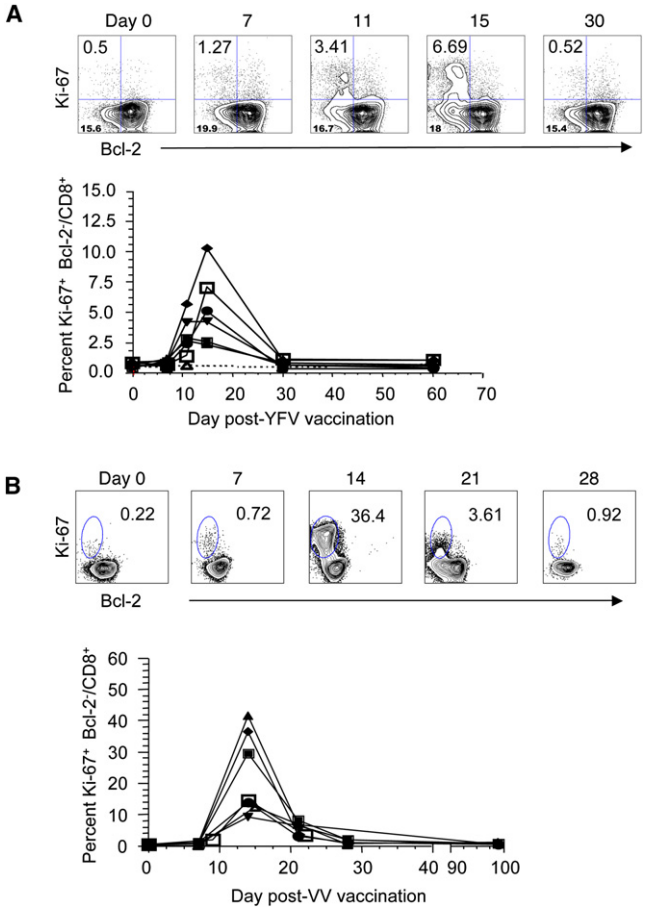

Figure 2. Identification of Proliferating and Proapoptotic CD8+ T Cells after Vaccination
Ki-67 and Bcl-2 expression in CD8+ T cells after YF-Vax (A) or Dryvax (B) immunization. Heparinized whole-blood samples from vaccine recipients were stained with antibodies against CD3, CD8, permeabilized, and subsequently stained for intracellular Ki-67 and Bcl-2 expression. FACS contour plots were gated on CD3+, CD8+ cells.

the activated Ki-67+ Bcl-2low phenotype (Figure 2A). The proportion of Ki-67+ Bcl-2low CD8+ T cells increased sharply after immunization. At the peak of the YF-vax response, 3%–11% of CD8+ T cells were Ki-67+, Bcl-2low. Similarly, 10%–40% of CD8+ T cells were Ki-67+, Bcl-2low at the peak of the T cell response to Dryvax immunization. In both cases, percentages of activated CD8+ T cells declined rapidly to background by day 30 after infection (Figure 2B).

The expression kinetics of Ki-67 and Bcl-2 on CD8+ T cells mirrored those of CD38 and HLA-DR. Indeed, we found that CD38+ CD8+ T cells were Ki-67+ and Bcl-2low, indicating that the combination of these markers effectively identified a recently generated population of activated T cells (Figure S1A available online). Because staining with these markers clearly identified an effector CD8+ T cell population, it also allowed us to analyze the expression patterns of other phenotypic markers on these activated CD8+ T cells. This led to a provisional phenotypic definition of effector cells as granzyme Bhigh, CCR5high, CCR7low, CD45RAlow, and CD62Lint (Figure S1B). Thus, immunization with the YF-Vax and Dryvax vaccines induced massive expansions of activated CD38+ HLA-DR+ Ki-67+ Bcl-2low CD8+ T cells. Dryvax immunization resulted in a 3- to 4-fold larger response than did YF-Vax immunization. However, the kinetics of the YF-Vax- and Dryvax-induced responses were similar. Activated CD8+ T cells were Ki-67+, consistent with massive expansion, and were susceptible to undergo apoptosis (Bcl-2low), consistent with the subsequent contraction phase of the response. Although the main conclusion from these experiments is that CD8+ T cell responses against live-attenuated vaccines are very large in magnitude, our data also illustrate that simple combinations of six markers (CD3, CD8, CD38, HLA-DR, Ki-67, and Bcl-2) can be used to identify effector T cell responses after immunization or infection.

Functional Characterization of Vaccine-Induced CD8+ T Cells

To correlate the observed expansions of activated CD8+ T cells with antigen-specific responses, we used intracellular

cytokine-staining assays in combination with antigen stimulation. YFV-specific responses were visualized by stimulation of PBMCs with YFV-infected SW-480 cells. The HLA-A2 allele was the only confirmed match between the stimulator cell line and the YF-Vax vaccine recipients. Thus, this assay measured at least the HLA-A2-restricted component of the total response. To assess VV-specific responses after Dryvax immunization, we infected PBMCs from vaccine recipients overnight with VV virus. Thus, whereas the YFV-stimulation assay only measured the HLA-A2-restricted fraction of the total response, the VV-stimulation assay was not restricted by HLA type.

YFV-specific CD8+ T cell responses were first identified by intracellular IFN-γ staining at day 7 after immunization and peaked at day 14, when 0.5%–3% of all CD8+ T cells secreted IFN-γ upon stimulation (Figure 3A). We observed a strong correlation between the frequency of IFN-γ-producing cells and the number of CD38+, HLA-DR+, Ki-67+, Bcl-2low CD8+ T cells (r^2 = 0.62 for IFN-γ+ versus CD38+ HLA-DR+ and r^2 = 0.67 for IFN-γ+ versus Ki-67+ Bcl-2low) (Figure S2A). To estimate the total YFV specific response, we stimulated PBMCs from vaccinated volunteers with matrix pools of overlapping 15-mer peptides that spanned the entire YFV polyprotein. An estimate of the total YFV-specific CD8+ T cell response was approximated by addition of the percentage of IFN-γ+ CD8+ cells in the 36 peptide pools that contained consecutive peptides. This analysis revealed that 2 months after vaccination, 0.1%–1.5% of CD8+ T cells were specific for YFV (Figure 3B). Frequencies of YFV-specific T cells slowly declined thereafter but were still detectable at frequencies ranging from 200–600 IFN-γ secreting cells per 10^6 PBMCs at 1 year after immunization (data not shown). We also observed a correlation between the peak expression of Ki-67+ CD8+ T cells at day 15 and the level of long-term YF-Vax-specific memory.

The VV-specific response kinetics were similar to the YFV response kinetics. By day 14 after vaccination, between 3% and 14% of CD8+ T cells produced IFN-γ upon VV stimulation (Figure 3C). VV-specific IFN-γ-producing cells were still detected at day 84 after immunization. As observed for YF-Vax, we found strong correlations between IFN-γ-producing cells and the frequencies of activated cells identified by CD38, HLA-DR, Ki-67, and Bcl-2 staining (r^2 = 0.88 for IFN-γ+ versus CD38+ HLA-DR+ and r^2 = 0.91 for IFN-γ+ versus Ki-67+ Bcl-2low) (Figure S2B). We did not detect intracellular tumor necrosis factor α (TNF-α) in the majority of IFN-γ-producing T cells. A possible explanation for this is that TNF-α production is not sustained during the 20 hr stimulation assay, in contrast to IFN-γ production (Slifka et al., 1999). Indeed, 6 hr stimulation of PBMCs with VV peptides (Terajima et al., 2003) generated primarily IFN-γ TNF-α double-positive CD8+ T cells (data not shown).

The kinetics of antigen-specific CD8+ T cell responses diverged from those visualized by the expression of activation markers in two respects. First, antigen-specific CD8+ T cells were detected beyond day 30 after immunization, whereas the proportion of activated effector CD8+ T cells (CD38+, HLA-DR+, Ki-67+, Bcl-2low) had returned to baseline levels at that point. This suggests that antigen-specific effector CD8+ T cells had lost their activated phenotype and differentiated into memory cells. Second, although the percentages of IFN-γ-producing CD8+ T cells strongly correlated with the percentages of CD38+, HLA-DR+ and Ki-67+, Bcl-2low CD8+ T cells at the peak of the response (Figures 1–3), they were consistently lower. The magnitude of the VV-specific CD8+ T cell response based on the IFN-γ assay accounted for approximately one-third of the total number of activated CD8+ T cells as determined by phenotypic analysis. The fact that the VV life cycle is blocked at an early stage in antigen-presenting cells (APCs) provides a potential explanation as it predicts that our assay will preferentially detect T cells specific for early antigens (Chahroudi et al., 2006). Indeed, a population of CD8+ T cells specific for an HLA-A2-restricted epitope in the putative early and late 189R gene open reading frame (Terajima et al., 2003) failed to produce IFN-γ after overnight VV stimulation (data not shown). However, it is possible that acute viral infections elicit a large population of bystander activated CD8+ T cells or that not all VV-specific T cells can produce cytokines in response to antigen stimulation.

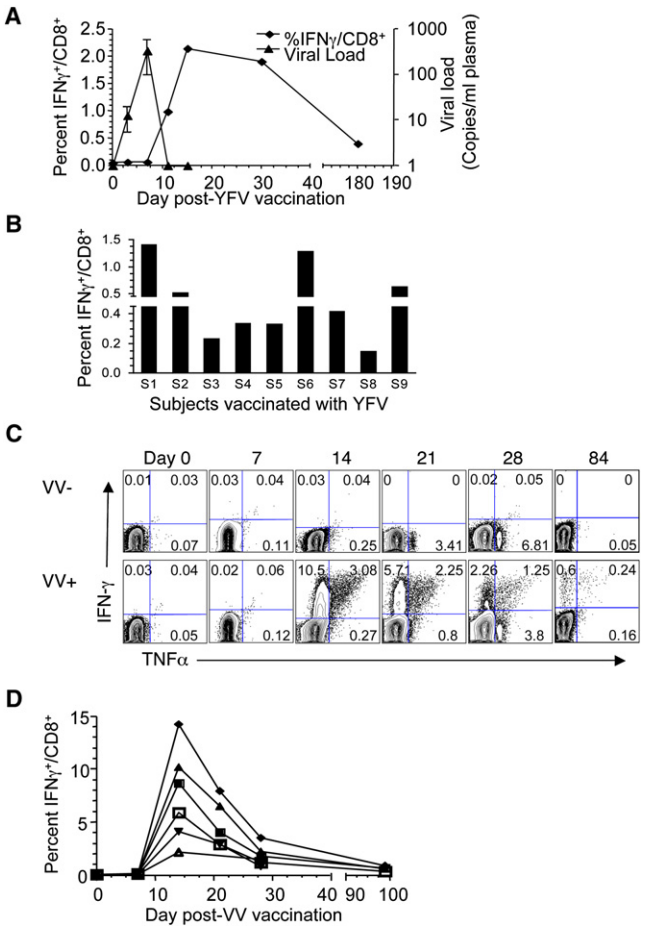

Figure 3. Kinetics of the YFV- and VV-Specific CD8+ T Cell Responses

(A) PBMCs from YFV-immunized donors, stimulated with YFV-infected SW-480 cells and analyzed for IFN-γ-producing cells.

(B) IFN-γ-producing CD8+ T cells in PBMCs from nine donors immunized 60 days before, stimulated with overlapping peptides spanning the YFV polyprotein. Error bars represent the standard error of the mean for three volunteers.

(C) PBMCs from Dryvax immunized donors stimulated with VV and analyzed for cytokine production.

(D) Percent of CD8+ T cells that produce IFN-γ in response to VV stimulation.

Minimal Bystander CD8+ T Cell Activation after YF-Vax or Dryvax Immunization

To evaluate possible CD8+ T cell bystander activation during acute viral infection, we analyzed how pre-existing nonvaccine-specific memory CD8+ T cells responded to immunization. Therefore, we monitored the activation status of the EBV-, CMV-, and/or influenza virus-specific CD8+ T cell populations that were present in multiple vaccine recipients. Responses of these unrelated memory CD8+ T cells after Dryvax and YF-Vax immunization were evaluated by analysis of the expression patterns of CD38, Ki67, and CD62L on unrelated memory CD8+ T cells, identified by MHC class I tetramer staining.

As shown in Figure 4A, we found that EBV-specific tetramer+ CD8+ T cells (HLA-A2 EBV^{RAK}) were neither activated nor proliferating (as defined by CD38 and Ki-67 upregulation, respectively) in response to YF-Vax immunization. However, in the same individual, we observed activated and proliferating CD8+ T cells in the tetramer-negative population, providing evidence of a strong YF-Vax induced response. Identical results were obtained with a CMV-specific tetramer (data not shown). Similarly, influenza virus (HLA-A2 INF^{GIL})-specific T cells in Dryvax-immunized volunteers did not upregulate CD38 or Ki-67 at any time after immunization (Figure 4B). In contrast, VV-specific CD8+ T cells (comprised within the tetramer-negative population) in the same individual dramatically upregulated CD38 and Ki-67 by day 15 after immunization (Figure 4B). Thus, we found no evidence for activation or for a proliferative response of unrelated CD8+ T cells after Dryvax or YF-Vax immunization. This suggests that bystander CD8+ T cell proliferation did not contribute to the massive expansion of effector T cells observed after vaccination.

In order to further determine the phenotypic nature of the EBV and influenza virus specific CD8+ T cell memory pools (i.e., effector or central memory) in immunized individuals, we also analyzed CD62L expression on tetramer+ EBV- and influenza virus-specific CD8+ T cells. This revealed that the EBV-specific memory CD8+ T cell pool predominantly consisted of $CD62L^{low}$ effector memory cells (76%) but also harbored $CD62L^{high}$ central memory cells (Figure 4A). The influenza virus-specific CD8+ memory T cell pool consisted almost exclusively of $CD62L^{high}$ central memory cells (Figure 4B). Because none of these memory cell populations displayed any bystander activation, our data imply that neither unrelated effector nor central memory cells were activated in a bystander fashion after YF-Vax or Dryvax immunization.

Combined, these results show that bystander activation of memory CD8+ T cells plays at most a limited role and does not contribute to the peak of the CD8+ T effector cell response after immunization. Thus, it is very likely that the observed effector CD8+ T cell responses to YF-Vax and Dryvax are mostly antigen specific.

Tracking VV-Specific CD8+ T Cell Responses with MHC Class I Tetramer

We used an MHC class I tetramer specific for an HLA-A2-restricted VV epitope, CLTEYILWV (Terajima et al., 2003), to further characterize the dynamics of the response and the phenotype of VV-specific effector and memory CD8+ T cells. HLA-A2 VV^{CLT} tetramer+ CD8+ T cells were detected in all 5 HLA-A2+ donors, ranging from 0.2% to 0.5% of total CD8+ T cells at the peak of

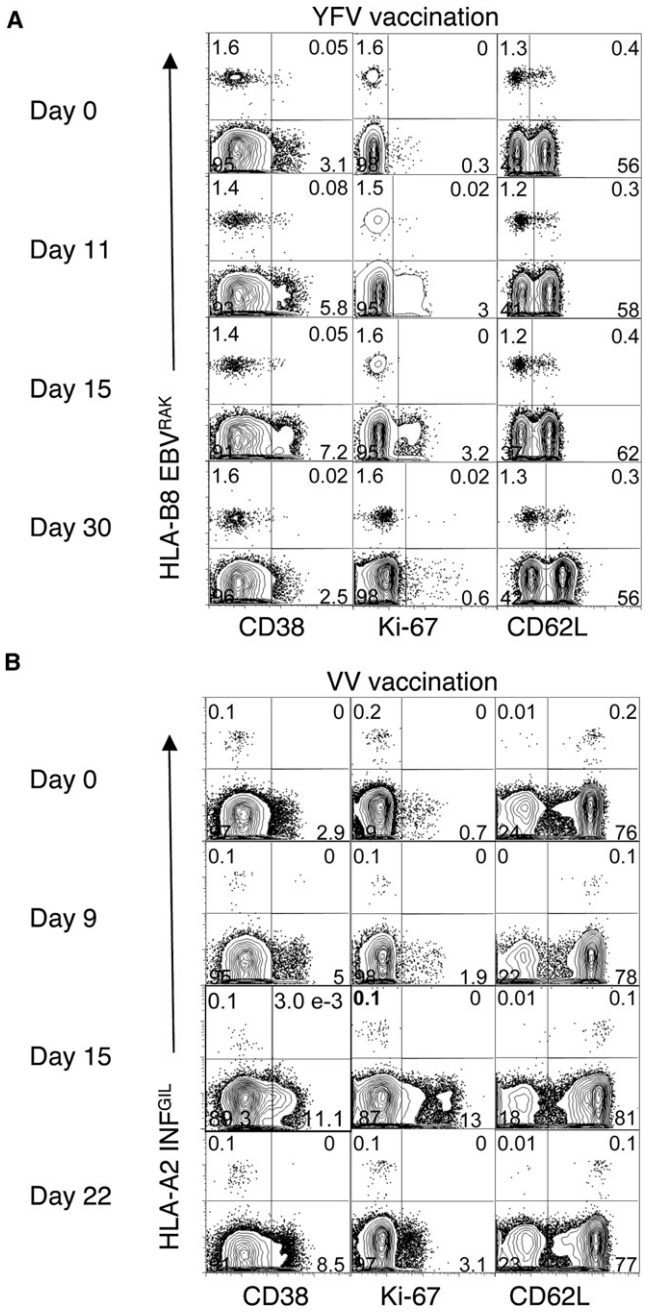

Figure 4. Analysis of Bystander CD8+ T Cell Activation after YF-VAX or Dryvax Vaccination

Heparinized whole-blood samples from YFV- and VV-immunized volunteers were stained with HLA-B8 EBV^{RAK} (A) or HLA-A2 INF^{GIL} (B) tetramers and antibodies against CD8, CD38, CD62L, and Ki-67. FACS plots are gated on CD8+ T cells.

the response (Figure 5A). The kinetics of HLA-A2 VV^{CLT+} CD8+ T cells (Figure 5B) were similar to the kinetics of activated ($CD38^+$ HLA-DR^+ Ki-67^+ Bcl-2^{low}) CD8+ T cells (Figure 3) and VV-specific IFN-γ-producing CD8+ T cells (Figure 3). This provides further evidence that the quantification of CD8+ T cell activation with this set of markers accurately predicts kinetics of the CD8+ T cell response to acute infection. The HLA-A2 VV^{CLT}

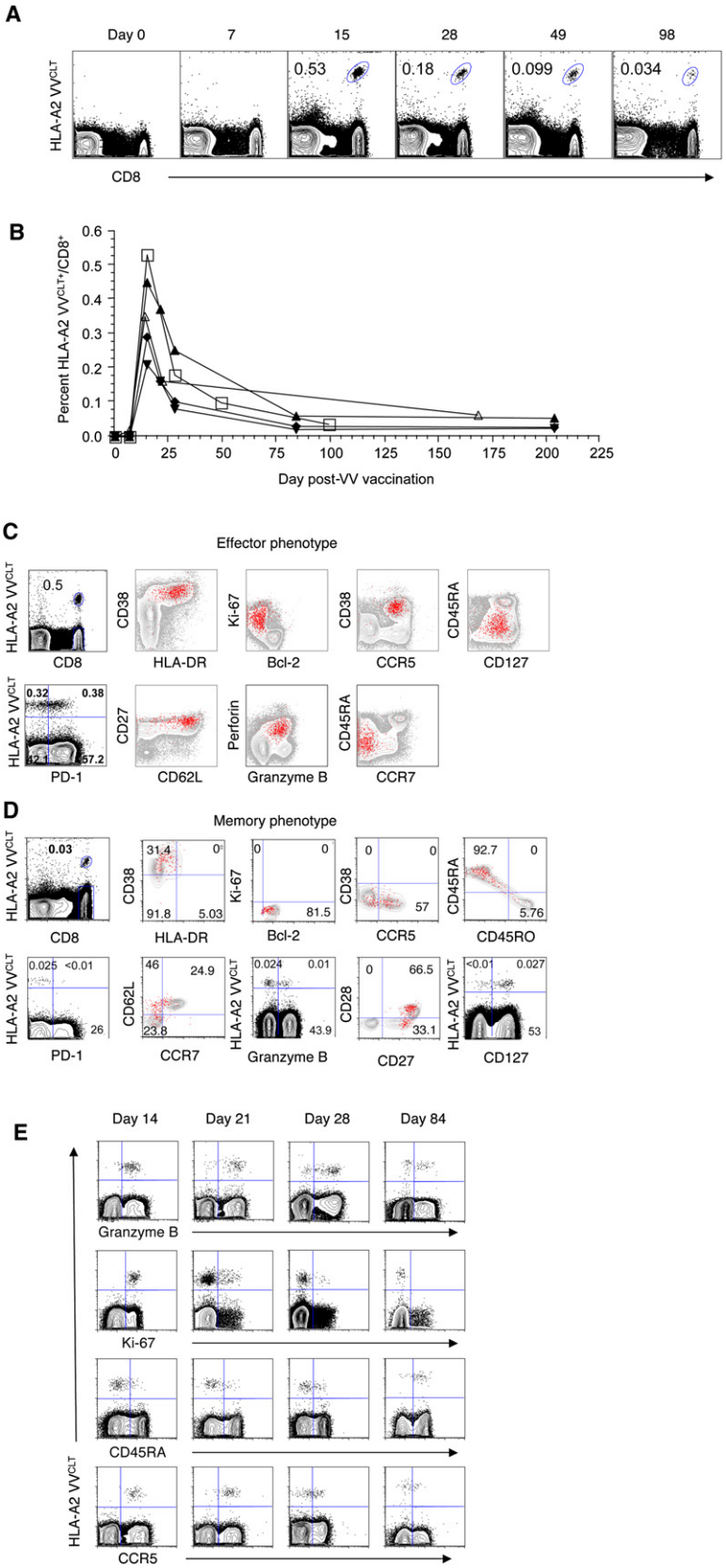

Figure 5. Tracking VV-Specific CD8+ T Cell Responses by MHC Class I Tetramer

(A) PBMCs from volunteers immunized with the smallpox vaccine were stained with HLA-A2 VV^{CLT} tetramer and antibodies against CD3 and CD8.

(B) The percentage of HLA-A2 VV^{CLT} tetramer-specific $CD8^+$ T cells as a proportion of total $CD8^+$ T cells were plotted over time for five vaccinated volunteers.

(C and D) HLA-A2 VV^{CLT} tetramer-specific effector and memory $CD8^+$ T cells at day 15 (C) and 6 months (D) after VV immunization were analyzed for the expression of various phenotypic markers. Antigen-specific $CD8^+$ T cells are depicted as red dots and total $CD8^+$ T cells as the gray background.

(E) Gradual effector-to-memory transition of VV antigen-specific cells after vaccination. Heparinized whole-blood was stained at multiple time points after smallpox vaccination with antibodies against Ki-67, granzyme B, CD45RA, CCR5, CD3, and CD8 and HLA-A2 VV^{CLT} tetramer. The plots shown are gated on $CD8^+$ T cells.

tetramer also allowed us to further define the phenotype of virus-specific effector (Figure 5C) and memory (Figure 5D) $CD8^+$ T cells.

At day 15 after immunization, HLA-A2 VV^{CLT} tetramer staining revealed a population of activated $CD45RO^+$ $CD8^+$ T cells characterized by the upregulation of CD38, CD27, HLA-DR, Ki-67, CCR5, perforin, and granzyme B and downregulation of Bcl-2, CCR7, and CD127 (Figure 5C). Consistent with previous data from mouse infection models, effector $CD8^+$ T cells also expressed Programmed Death 1 (PD-1). Surprisingly however, tetramer$^+$ effector $CD8^+$ T cells were also $CD62L^{int}$. These findings are consistent with the effector T cell phenotype deduced from bulk T cell staining after YF-Vax immunization (Figure S1). Expression of perforin and granzyme B, hallmarks of effector T cells, indicates that all tetramer$^+$ $CD8^+$ T cells possess high cytolytic potential at the peak of the effector T cell response.

By using the VV^{CLT} tetramer, we then analyzed the phenotype of VV-specific memory $CD8^+$ T cells. Six months after Dryvax immunization, we detected HLA-A2 VV^{CLT}-specific T cells at 0.03% of total $CD8^+$ T cells (Figure 5D). At this point, most antigen-specific cells had undergone further differentiation and no longer exhibited an effector phenotype (Figure 5D). Tetramer$^+$ memory HLA-A2 VV^{CLT+} T cells were $CD45RA^+$ and $CD27^+$, had downregulated CD38, HLA-DR, and Ki-67, and re-expressed Bcl-2 and CD127. Bimodal expression patterns were observed for CCR5, CCR7, CD62L, CD28, and granzyme B. Memory $CD8^+$ T cells had downregulated PD-1 expression, consistent with their full functionality and clearance of virus (Figure 5D). This result suggests that antigen stimulation is required to maintain PD-1 expression on memory $CD8^+$ T cells. The phenotype that we describe here was observed in all donors that possessed HLA-A2 VV^{CLT}-specific T cells (n = 5). The bimodal expression patterns of granzyme B, CCR5, CCR7, CD62L, and CD28 suggest that memory T cell populations may be further subdivided on the basis of their homing marker expression and cytotoxic potential.

Effector-to-Memory $CD8^+$ T Cell Transition after Vaccination

On the basis of the distinct phenotypes of effector and memory $CD8^+$ T cells, we asked whether the transition from an effector to a memory cell phenotype would be an abrupt or gradual event and whether this transition would occur simultaneously for different markers. To address this question, we analyzed the expression patterns of a selected set of markers (Ki-67, CD45RA, CCR5, and granzyme B) on tetramer$^+$ $CD8^+$ T cells at multiple time points after immunization (days 15, 21, 28, and 84). As shown in Figure 5E, differentiation from effector to memory phenotype happened gradually over several weeks of time. Interestingly, effector-to-memory transition did not progress simultaneously for all markers. For instance, Ki-67 downregulation was an early event with most tetramer$^+$ cells downregulating Ki-67 expression by day 21 after immunization. In contrast, the change from CD45RO to CD45RA and the downregulation of granzyme B occurred with slower kinetics. Thus, tetramer$^+$ T cells displayed effector-like expression of granzyme B and CD45RA at 28 days after infection but were no longer proliferating (Ki-67) and displayed different migration properties (CCR5). Combined, these data suggest that antigen-specific $CD8^+$ T cells pass through several phenotypic stages after the peak of the effector response. However, the nonsimultaneous, gradual changes in the expression patterns of several key markers suggest that effector-to-memory $CD8^+$ T cell differentiation is a continuous, linear process and not a succession of discrete phenotypic stages.

At 2 years after immunization, $CD45RA^+$ tetramer$^+$ $CD8^+$ T cells were still detectable in the blood at a frequency of 0.012% of $CD8^+$ T cells (data not shown). Expression of CD45RA has been proposed as a surrogate marker for terminally differentiated memory $CD8^+$ T cells, with limited proliferative potential (Champagne et al., 2001). To test whether this phenotype applied to VV-specific CD45RA memory cells, we stimulated 5,6-carboxy fluorescein diacetate succinimidyl ester (CFSE)-labeled PBMCs with the VV^{CLT} peptide. Clearly, after 6 days of stimulation with peptide, HLA-A2 VV^{CLT+} T cells underwent multiple rounds of proliferation (Figure 6A). CD45RA memory cells also produced IFN-γ and IL-2 after 6 hr peptide stimulation (Figure 6B). These results suggest that $CD45RA^+$ memory T cells are not terminally differentiated and maintain the potential to proliferate and secrete effector cytokines in response to antigen. Similar results were obtained when PBMCs from YF-Vax immunized volunteers were stimulated with a pool of five peptides (Co et al., 2002): YFV-specific $CD8^+$ T cells displayed extensive proliferation (Figure 6A) and produced IFN-γ and IL-2 upon antigenic stimulation (Figure 6B).

$CD4^+$ T Cell and B Cell Responses after Drvax Vaccination

In order to determine how the VV-specific $CD8^+$ T cell response relates to the other major components of the adaptive immune system, the VV-specific $CD4^+$ T cell response and the neutralizing antibody titer were compared in the same subjects (Figure 7). VV-neutralizing antibodies were detected by day 15 after vaccination and were maintained at high levels. The magnitude of the VV-specific $CD4^+$ T cell response was measured by IFN-γ production in response to vaccinia virus stimulation of donor PBMCs in vitro. The kinetics of the $CD4^+$ T cell response paralleled the VV-specific $CD8^+$ T cell response. However, it was one-half to one-third of the magnitude of the VV-specific CD8 T cell response. It is worth noting that the ratio of virus-specific CD8 versus CD4 T cell responses seen in humans after Dryvax immunization was strikingly similar to the results seen in mice after VV infection, where the CD8 T cell responses were again higher in magnitude than the CD4 T cell responses (Harrington et al., 2002). In summary, the data in Figure 7 show that $CD8^+$ T cell responses after smallpox vaccination occur in concert with $CD4^+$ T cell and B cell responses and that all of these primary T and B cell responses occur very rapidly.

DISCUSSION

Longitudinal studies of host immune responses after the onset of infection are crucial to understanding of the generation and maintenance of antigen-specific effector and memory T cells in humans. To explore the human $CD8^+$ T cell response to acute infection, we performed a longitudinal analysis of $CD8^+$ T cells responding to the live YFV and smallpox (vaccinia virus) vaccines—two of the most successful human vaccines ever developed. Our study makes four distinct points. First, we

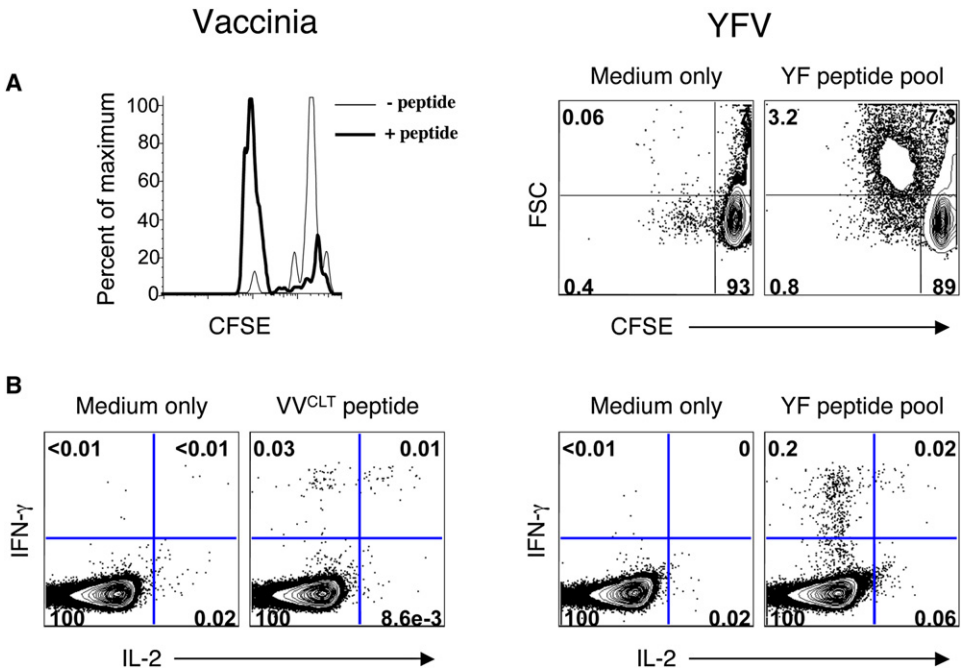

Figure 6. Functional Analysis of VV- and YFV-Specific Memory CD8+ T Cells

(A) PBMCs from VV- and YFV-vaccinated donors at 2 years or 90 days after vaccination, respectively, were labeled with CFSE and stimulated in the presence or absence of VV^{CLT} peptide or YFV peptide pools for 6 days. Proliferation was measured by dilution of the CFSE dye as analyzed by flow cytometry. The VV histogram is gated on HLA-VV^{CLT} tetramer-specific $CD8^+$ T cells. YFV plots are gated on $CD3^+$ $CD8^+$ lymphocytes.

(B) PBMCs from VV- and YFV-vaccinated donors were stimulated in the presence or absence of VV^{CLT} peptide or YFV peptide pools for 6 hr and cells were stained for intracellular cytokine levels. The data shown are gated on $CD3^+$ $CD8^+$ T cells.

show that the expression patterns of the activation markers HLA-DR, CD38, Ki-67, and Bcl-2 could be used to identify the newly generated effector $CD8^+$ T cells. This simple phenotypic analysis should be broadly applicable to quantify effector T cells after immunization or infection. Second, both vaccines induced a brisk primary effector T cell response of substantial magnitude that was readily detectable within 2 weeks of infection. At the peak of the primary response, YFV- and VV-induced effector $CD8^+$ T cells accounted for up to 12.5% and 40% of $CD8^+$ T cells in the blood, respectively. Third, by monitoring the responses of pre-existing memory $CD8^+$ T cells to unrelated pathogens, we show that there was minimal to no bystander activation or proliferation after YFV or VV immunization and that the majority of the responding T cells are likely to be specific to the vaccine. Fourth, phenotypic analysis of MHC class I tetramer$^+$ $CD8^+$ T cells indicated that (1) virus-specific $CD8^+$ T cells pass through an obligate effector phase defined by the expression of perforin and granzyme B, (2) effector T cells contracted to approximately 10% of the peak and then gradually differentiated into a long-lived pool of memory cells, and (3) memory $CD8^+$ T cells generated after acute VV or YFV infection exhibited phenotypic and functional characteristics distinct from those described for human $CD8^+$ T cells specific for persistent viruses.

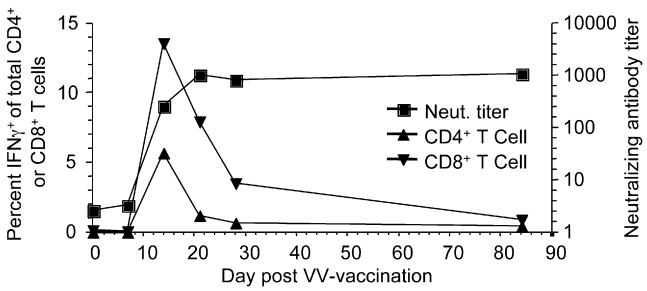

Figure 7. Kinetics of $CD4^+$ and $CD8^+$ T Cell and Neutralizing Antibody Responses to Dryvax Vaccine

The percentage of IFN-γ-producing $CD4^+$ and $CD8^+$ T cells and the VV-neutralizing antibody titers for a single donor after Dryvax immunization were plotted over time. These data are representative of responses observed in other individuals.

We used a combination of four phenotypic markers (CD38, HLA-DR, Ki-67, and Bcl-2) to identify a discrete population of activated effector $CD3^+$ $CD8^+$ T cells. We propose that this population truly represents the antigen-specific T cells response. This implies that simple phenotypic analysis can be used to assess T cell responses without prior knowledge of antigenic specificity. We predict that with the simultaneous use of four markers to visualize a single population of T cells, even much weaker responses can be rapidly visualized. In addition, these markers can be utilized during vaccine trials to more specifically determine the quality of $CD8^+$ priming and differentiation.

The magnitude of antiviral $CD8^+$ T cell response, as estimated by phenotypic analysis, ranged from 2% to 13% for YF-Vax and 10% to 40% of $CD8^+$ T cells for Dryvax at the peak of the T cell response. Functional analyses (IFN-γ staining) could account for only one-third of the total response, but this probably reflects limitations of the stimulation protocols that we used. It is also possible that not all virus-specific $CD8^+$ T cells respond by

IFN-γ production. Nevertheless, the total numbers of $CD8^+$ T cells involved in these responses are very high. On the basis of a total estimated number of 3×10^{11} $CD8^+$ T cells in humans (Boon et al., 2006), we estimate that at the peak of the response (2 weeks), between 9×10^9 and 4.2×10^{10} $CD8^+$ T cells were VV specific and between 1.5×10^9 and 9×10^9 $CD8^+$ T cells were YFV specific, on the basis of IFN-γ production. On the basis of phenotypic staining, the total number of activated $CD8^+$ T cells could be as much as 1.2×10^{11} cells (40%) and 3.8×10^{10} for Dryvax and YF-Vax, respectively. Assuming an approximate precursor frequency of $1/10^5$ to $1/10^6$ naive T cells, this corresponded up to a 10^4- to 10^5-fold expansion of IFN-γ^+ T cells, or up to 16–20 cell divisions. These results parallel studies in murine models where $CD8^+$ T cells undergo up to 15 rounds of proliferation in vivo during an acute viral infection (Murali-Krishna et al., 1998).

The peak of the $CD8^+$ effector T cell response occurred within 2 weeks after YF-Vax or Dryvax immunization. For both vaccines, effector responses declined to background by 4 weeks after inoculation. Similar kinetics were observed for $CD4^+$ T cells and neutralizing antibody titers. In contrast, T and B cell responses to chronic infections (such as HIV, HBV, and HCV) can take much longer to develop after infection (Forns et al., 2000; Sakai et al., 2007; Thimme et al., 2002; Thimme et al., 2003). Thus, our experiments reveal very different response kinetics in acute versus chronic infection settings. It is tempting to speculate that the rapid response to Dryvax or YF-Vax immunization represents the optimal response, whereas slower responses are suboptimal and may be causally related to viral persistence.

VV-specific tetramer$^+$ cells contracted more than 90% by day 84 after infection. Assuming similar contraction kinetics for all VV-specific T cells, we estimate that the memory pool at this time point contained approximately 1×10^9 VV-specific memory $CD8^+$ T cells. In the absence of antigen, we detected a further decline in tetramer$^+$ memory cells. From 3 months to 2 years after infection, we observed an approximately 60% reduction in antigen-specific cells. Assuming that this loss in the memory phase was constant and linear over time, this means that the size of the HLA-A2 VV^{CLT}-specific memory population will exceed the size of the precursor pool for at least 12 years and that tens of thousands of memory cells, capable of immediate recall responses, will survive over 20 years. In fact, we were able to detect bulk VV-specific T cells by IFN-γ secretion in individuals that were vaccinated more than 50 years prior (data not shown). This suggests that $CD8^+$ T cell burst size is one of the biological determinants that may be responsible for long-term protective immunity of the Dryvax and YF-Vax vaccines.

The role of bystander activation during antiviral T cell responses has been a long-standing and controversial issue (Butz and Bevan, 1998; Callan et al., 1998; Ehl et al., 1997; McNally and Welsh, 2002; Murali-Krishna et al., 1998; Tough et al., 1996; Tough and Sprent, 1998; Zarozinski and Welsh, 1997). Previous studies suggested that nonspecific $CD8^+$ T cells can display an activated phenotype and perform cytolytic T cell functions in the apparent absence of T cell receptor (TCR) engagement (Ehl et al., 1997; Tough et al., 1996). However, with the advent of MHC tetramer technology, it is now clear that the massive expansions of effector $CD8^+$ T cells in murine LCMV infections and human EBV infections (infectious mononucleosis) are mostly antigen specific (Callan et al., 1998; Murali-Krishna et al., 1998; Tan et al., 1999). This suggests that TCR engagement is the primary driving force behind the activation of antiviral $CD8^+$ T cells but does not disprove a possible, albeit small, role for bystander activation. However, by using MHC class I tetramers for EBV-, CMV-, and influenza-specific $CD8^+$ T cells, we found that unrelated memory $CD8^+$ T cells do not contribute to the peak of the VV- and YF-Vax-specific $CD8^+$ T cell response, either by upregulation of activation markers or by proliferation. Interestingly, we did detect some activation of EBV-specific $CD8^+$ T cells in vaccine recipients at day 21 after Dryvax immunization, although influenza-specific $CD8^+$ T cells in the same individuals did not show any changes in number or phenotype (data not shown). On the basis of the kinetics and EBV specificity of this phenomenon, this result likely reflects the reactivation of latent EBV in response to Dryvax immunization (Doisne et al., 2004; Lechner et al., 2000). A similar phenomenon was recently described in individuals acutely infected with Puumala virus (Tuuminen et al., 2007). Combined, these data suggest that the large populations of effector T cells observed at the peak of the response are specific for VV or YFV antigens and that TCR engagement is a prerequisite for activation of antigen-specific $CD8^+$ T cells. This implies that memory $CD8^+$ T cells are unlikely to be maintained by bystander activation as a result of a heterologous infection (i.e., without TCR engagement). Thus, long-term T cell memory appears to be maintained in the absence of antigenic stimulation, although there is most likely a slow decline over time.

MHC class I tetramer staining allowed us to define detailed effector and memory $CD8^+$ T cell phenotypes. Consistent with their function, effector $CD8^+$ T cells expressed Ki-67 (proliferation), granzyme B, and perforin (cytolytic activity) and downregulated Bcl-2 (prone to undergo apoptosis). Transient PD-1 expression was observed, similar to results from murine infection models. These data support a model in which primed effector cells exit lymph nodes by downregulating CCR7, migrate to infected tissues via CCR5, and kill infected cells by secreting perforin and granzyme. A surprising finding was that the majority of effector $CD8^+$ T cells were $CD62L^{int}$, whereas T cell activation is usually associated with CD62L downregulation (Callan et al., 1998; Wherry et al., 2003b). This lack of downregulation did not result from an intrinsic defect because VV-specific $CD62L^{high}$ $CD8^+$ T cells rapidly downregulated CD62L upon in vitro restimulation (data not shown). CD62L downregulation has previously been described in patients with chronic or persistent infections (Callan et al., 1998), and it is possible that the lack of CD62L downregulation in our experiments reflects the differences between acute and chronic viral infections, e.g., antigen load, duration of antigen exposure, and impairment of T cell function in the setting of chronic antigen exposure.

The effector molecules perforin and granzyme B were expressed by all HLA-$A2^{CLT}$ tetramer$^+$ $CD8^+$ T cells at the peak of the response (day 14), consistent with recently published data (Precopio et al., 2007). This indicates that antiviral $CD8^+$ T cells pass through an obligate effector phase before differentiating into memory cells, suggesting a linear effector-to-memory differentiation model. The phenotypic changes that accompanied passage from the effector to memory phase occurred gradually

over a period of several weeks and at distinct rates for different markers. For example, Ki-67 downregulation was an early event, whereas downregulation of granzyme B and CCR5 happened more slowly. Also, the transition from effector to memory phenotype was associated with a gradual change from $CD45RO^+$ to $CD45RA^+$ (Carrasco et al., 2006). Thus, whereas effector and memory cells were strictly $CD45RO^+$ and $CD45RA^+$, respectively, more complex phenotypes existed in the transition phase. Altogether, these data support a model of linear differentiation where naive cells expand and differentiate into effector cells after antigen stimulation and then contract and slowly differentiate into a stable population of memory cells.

The VV-specific ($HLA\text{-}A2^{CLT}$ tetramer$^+$) memory $CD8^+$ T cell pool itself was phenotypically diverse. Memory cells expressed CD45RA and CD27 and were characterized by downregulation of activation markers such as Ki-67, CD38, HLA-DR, and PD-1 and bimodal expression of CCR7, CCR5, CD62L, CD28, and granzyme B. The bimodal expression patterns of multiple homing markers suggest that the memory cell population may be subdivided on the basis of lymphoid and tissue homing capabilities, consistent with the central and effector memory concept. Memory cells expressed the IL-7 receptor CD127, similar to HIV- and RSV-specific memory cells and previously reported VV data, suggesting that IL-7 signaling plays a role in the homeostatic maintenance of memory populations (Kaech et al., 2003). At 6 months after immunization, we observed small populations of $CD127^{low}$ VV-specific $CD8^+$ T cells, possibly representing memory cells that had recently received IL-7 signals (Vranjkovic et al., 2007). The memory phenotype that we describe here seems to differ slightly from the recently described $CD45RA^+$ $CD27^{int}$ VV-specific $CD8^+$ T cells, detected at 1 month after Dryvax immunization. According to our data, CD45RO- and CD45RA-expressing memory T cells coexist at this time. However, close inspection of the data reported by Precopio et al. (2007) suggests that $CD45RO^+$ cells were still detected at 1 month after immunization. Combined, these data support our conclusion that effector-to-memory differentiation is a gradual and continuous process.

The phenotype of VV-specific memory cells does not entirely correlate with the current differentiation models proposed for human memory $CD8^+$ T cells. For example, Champagne et al. (2001) and Sallusto et al. (1999) have defined $CD45RA^+$ $CCR7^-$ $CD8^+$ T cells as terminally differentiated and unable to undergo substantial proliferation upon antigenic stimulation. This is clearly different from our present data. The obvious variable that could explain these differences is that we describe a memory phenotype in the context of acute rather than chronic infection. Transient viremia (as observed for YF-Vax) implies that the transition from effector to memory cells occurs in the absence of antigenic stimulation. In contrast, the effector-to-memory transition during chronic infection is most likely associated with persistent TCR stimulation. This difference in the persistence and degree of TCR signaling may differentially affect the maturation pathway of responding $CD8^+$ T cells during acute and chronic infections, resulting in distinct cellular phenotypes and functional capacities. Thus, persistent antigen exposure during the memory-formation phase could lead to different, and possibly less functional, $CD8^+$ memory T cells. This implies that vaccine boosting should occur after the formation of a phenotypically stable population of memory cells. Furthermore, drug therapies aimed at reducing viral loads during the early stages of chronic infections may result in the formation of more effective immune memory.

In conclusion, we report that human $CD8^+$ T cell responses to acute viral infections are very large and can be visualized in a nonantigen-specific way by the simple combination of four activation markers. The collective evidence suggests that the response identified by these markers is the true antiviral response and that bystander activation only plays a minimal role in this context. Tetramer staining data exposed distinct effector and memory $CD8^+$ T cell phenotypes and also revealed that the effector-to-memory transition is a gradual and linear process, associated with multiple phenotypic changes. Taken together, these results provide a benchmark for the $CD8^+$ T cell response induced by two highly successful human vaccines and provides insight into human memory T cell differentiation after acute viral infection.

EXPERIMENTAL PROCEDURES

Vaccine Immunizations

After receipt of informed consent, healthy volunteers were screened for expression of HLA-A2. Ten male and female healthy volunteers (ranging in age from 21 to 32 years) found to be HLA-A2 positive were administered the live-attenuated YFV-17D vaccine (YF-Vax, sanofi pasteur) or the live vaccinia smallpox vaccine (Dryvax, Wyeth Laboratories) according to the product label. YF-Vax was administered subcutaneously in the arm with no less than 4.74 $\log_{10}$ plaque-forming units per 0.5 ml dose. Dryvax was administered by scarification in the upper arm with three pricks of a bifurcated needle (estimated dose 2.5×10^5 PFU).

Study Subjects and Blood Samples

This study protocol was reviewed and approved by the Emory University Human Investigations Committee. Volunteer screening, vaccination, and collection of blood samples were done in close collaboration with the Hope Clinic of the Emory Vaccine Center. Exclusion criteria for vaccination followed recommendations established by the Advisory Committee on Immunization Practices (ACIP) and the YF-Vax and Dryvax product labels. Blood samples were obtained from the volunteers at baseline and at sequential times after vaccination. Samples were obtained at days 0, 3, 7, 11, 15, and 30 after YF-Vax immunization or at days 0, 7, 14, 21, 28, and 84 after Dryvax immunization. Slightly different schedules were employed for some donors, as indicated in the text. Seroconversion after vaccination was confirmed by assaying of the neutralizing antibody titers for YFV-17D and VV (data not shown). PBMCs were purified by Ficoll-Hypaque density gradient centrifugation of heparinized blood samples or with CPT tubes. EDTA blood samples were used to quantify viral RNA.

Reagents

All monoclonal antibodies were obtained from BD PharMingen (San Diego, CA). $HLA\text{-}A2\ INF^{GIL}$, $HLA\text{-}B8\ EBV^{RAK}$, $HLA\text{-}A2\ EBV^{GLC}$, and $HLA\text{-}A2\ VV^{CLT}$ tetramers were made as previously described (Miller et al., 2003). The WR strain of vaccinia virus was obtained from the ATCC. SW480 cells were obtained from the ATCC, and the YFV-17D used for in vitro infection originated from infectious transcripts made from the full-length complementary DNA (cDNA) clone, as described previously (Rice et al., 1989).

Staining and Flow Cytometry

The appropriate antibodies were added to 150–500 μl whole blood and incubated at room temperature for 30 min, and 10 min lysis of red blood cells with FACS Lysing Solution (BD PharMingen) followed. For intracellular staining, cells were permeabilized with FACS Permeabilization solution (BD PharMingen) and incubated with antibodies against Bcl-2, Ki-67, granzyme B, and perforin. Samples were analyzed on a FACScalibur flow cytometer (BD PharMingen) and analyzed with Flowjo (Treestar, Ashland, OR) software.

YFV-17D Peptide Library

The YFV-17D peptide synthesis and their organization into peptide pools were done on the basis of methods described by Hoffmeister et al. (2003). The library consisted of 15 amino acid long nonamidylated peptides (SynPep, Dublin, CA) spanning the entire YFV-17D polyprotein; consecutive peptides overlapped by 11 amino acids. The 851 peptides comprising the library were organized into 60 pools based on a 24 × 30 matrix with each pool containing 24 to 30 peptides.

Yellow Fever Stimulation Assays

PBMCs were stimulated with either with peptide pools (with each peptide at a concentration of 10 μg/ml) or SW-480 cells that had been infected with YFV-17D (multiplicity of infection [m.o.i.] 1, used at 48 hr after infection) or mock infected at a ratio of 1:1. For intracellular cytokine staining experiments, 500,000 PBMCs were incubated with 500,000 SW-480 cells for 6 hr in the presence of brefeldin A. After the incubation, cells were fixed with FACS lysing solution (BD PharMingen), permeabilized (FACS Permeabilization solution, BD PharMingen), and incubated with antibodies against CD3, CD8, IFN-γ, and TNF-α. Flow cytometry and analysis were performed as described above. For the in vitro CFSE dilution assay, 1–2 × 10^7 PBMCs were labeled with 3 μM CFSE for 5 min, washed, and resuspended in RPMI containing 10% fetal calf serum (FCS). The labeled cells were stimulated in a 24-well plate with a pool of five YFV-17D-specific peptides. Medium was replaced 3 days after culture, and the CFSE dilution was analyzed by flow cytometry after a total incubation of 6 days.

Vaccinia Virus Stimulation Assays

PBMCs were stimulated for 15 hr with live WR strain of vaccinia virus (ATCC, Manassas, VA) at an m.o.i. of 1. After the 15 hr incubation at 37°C, Brefeldin A was added and the cultures were incubated for an additional 5 hr. The cells were then stained for CD3 and CD8 surface antigens as described above. Cultures were then fixed and permeabilized with a cytofix and cytoperm kit (BD PharMingen) and stained for intracellular IFN-γ and TNF-α. Flow cytometry and analysis were performed as described above. In vitro proliferation with CFSE dilution was done as described for YFV-17D with HLA-A2 VV^{CLT} peptide for stimulation instead of YFV-17D peptides.

YFV-Specific Real-Time PCR

YFV in the blood of vaccinees was obtained with a TaqMan real-time polymerase chain reaction (PCR) assay (Applied Biosystems, Foster City, CA). The following primers were used: 5′-CTACGTGTCTGGAGCCCGCAGCAAT-3′ (FAM- and TAMRA-labeled TaqMan probe), 5′-GAACAGTGATCAGGAACCCTCTCT-3′ (Fwd primer), and 5′-GGATGTTTGGTTCACAGTAAATGTG-3′ (Rev primer).

Primers for real-time PCR were designed within the highly conserved nonstructural NS5 gene of YFV with Primer Express software (Applied Biosystems). RNA was isolated from plasma samples with a QIAamp viral RNA minikit (QIAGEN, Netherlands). The two-step reverse transcriptase (RT)-PCR was performed with a TaqMan Gold kit under the following conditions: The 50 μl reactions contained 5 μl of 10× TaqMan buffer A, 4 mM $MgCl_2$, 400 μM dNTPs, a 200 nM concentration of each primer, a 125 nM concentration of the fluorogenic probe, 2.5 μM of random hexamer, 1.25 units of AmpliTaq Gold DNA polymerase (Applied Biosystems), 20 units of recombinant Mo-MuLV MultiScribe, and 8 units of RNase inhibitor in 20 μl volume for reverse transcription. Thermal cycling conditions consisted of 10 min at 25°C, 20 min at 42°C, 5 min at 99°C (first step), 10 min at 95°C, and then 45 cycles of 15 s at 95°C and 1 min at 60°C. Absolute quantification of RNA transcripts was determined with RNA template standards.

Detection of Neutralizing Antibodies

Serum-neutralizing antibody titers were determined as previously described (Newman et al., 2003).

SUPPLEMENTAL DATA

Two figures are available at http://www.immunity.com/cgi/content/full/28/5/710/DC1/.

ACKNOWLEDGMENTS

The authors would like to thank E. J. Wherry, S. Kaech, and S. Crotty for helpful discussions.

Received: October 4, 2007
Revised: February 25, 2008
Accepted: February 28, 2008
Published online: May 8, 2008

REFERENCES

Amara, R.R., Nigam, P., Sharma, S., Liu, J., and Bostik, V. (2004). Long-lived poxvirus immunity, robust CD4 help, and better persistence of CD4 than CD8 T cells. J. Virol. *78*, 3811–3816.

Appay, V., Dunbar, P.R., Callan, M., Klenerman, P., Gillespie, G.M., Papagno, L., Ogg, G.S., King, A., Lechner, F., Spina, C.A., et al. (2002). Memory CD8+ T cells vary in differentiation phenotype in different persistent virus infections. Nat. Med. *8*, 379–385.

Barber, D.L., Wherry, E.J., Masopust, D., Zhu, B., Allison, J.P., Sharpe, A.H., Freeman, G.J., and Ahmed, R. (2006). Restoring function in exhausted CD8 T cells during chronic viral infection. Nature *439*, 682–687.

Barouch, D.H., and Letvin, N.L. (2001). CD8+ cytotoxic T lymphocyte responses to lentiviruses and herpesviruses. Curr. Opin. Immunol. *13*, 479–482.

Becker, T.C., Wherry, E.J., Boone, D., Murali-Krishna, K., Antia, R., Ma, A., and Ahmed, R. (2002). Interleukin 15 is required for proliferative renewal of virus-specific memory CD8 T cells. J. Exp. Med. *195*, 1541–1548.

Boon, T., Coulie, P.G., Van den Eynde, B.J., and van der Bruggen, P. (2006). Human T cell responses against melanoma. Annu. Rev. Immunol. *24*, 175–208.

Butz, E.A., and Bevan, M.J. (1998). Massive expansion of antigen-specific CD8+ T cells during an acute virus infection. Immunity *8*, 167–175.

Callan, M.F., Tan, L., Annels, N., Ogg, G.S., Wilson, J.D., O'Callaghan, C.A., Steven, N., McMichael, A.J., and Rickinson, A.B. (1998). Direct visualization of antigen-specific CD8+ T cells during the primary immune response to Epstein-Barr virus In vivo. J. Exp. Med. *187*, 1395–1402.

Carrasco, J., Godelaine, D., Van Pel, A., Boon, T., and van der Bruggen, P. (2006). CD45RA on human CD8 T cells is sensitive to the time elapsed since the last antigenic stimulation. Blood *108*, 2897–2905.

Chahroudi, A., Garber, D.A., Reeves, P., Liu, L., Kalman, D., and Feinberg, M.B. (2006). Differences and similarities in viral life cycle progression and host cell physiology after infection of human dendritic cells with modified vaccinia virus Ankara and vaccinia virus. J. Virol. *80*, 8469–8481.

Chakrabarti, L.A., Lewin, S.R., Zhang, L., Gettie, A., Luckay, A., Martin, L.N., Skulsky, E., Ho, D.D., Cheng-Mayer, C., and Marx, P.A. (2000). Normal T-cell turnover in sooty mangabeys harboring active simian immunodeficiency virus infection. J. Virol. *74*, 1209–1223.

Champagne, P., Ogg, G.S., King, A.S., Knabenhans, C., Ellefsen, K., Nobile, M., Appay, V., Rizzardi, G.P., Fleury, S., Lipp, M., et al. (2001). Skewed maturation of memory HIV-specific CD8 T lymphocytes. Nature *410*, 106–111.

Co, M.D., Terajima, M., Cruz, J., Ennis, F.A., and Rothman, A.L. (2002). Human cytotoxic T lymphocyte responses to live attenuated 17D yellow fever vaccine: Identification of HLA-B35-restricted CTL epitopes on nonstructural proteins NS1, NS2b, NS3, and the structural protein E. Virology *293*, 151–163.

Crotty, S., Felgner, P., Davies, H., Glidewell, J., Villarreal, L., and Ahmed, R. (2003). Cutting edge: Long-term B cell memory in humans after smallpox vaccination. J. Immunol. *171*, 4969–4973.

Demkowicz, W.E., Jr., and Ennis, F.A. (1993). Vaccinia virus-specific CD8+ cytotoxic T lymphocytes in humans. J. Virol. *67*, 1538–1544.

Demkowicz, W.E., Jr., Littaua, R.A., Wang, J., and Ennis, F.A. (1996). Human cytotoxic T-cell memory: Long-lived responses to vaccinia virus. J. Virol. *70*, 2627–2631.

Doisne, J.M., Urrutia, A., Lacabaratz-Porret, C., Goujard, C., Meyer, L., Chaix, M.L., Sinet, M., and Venet, A. (2004). CD8+ T cells specific for EBV,

cytomegalovirus, and influenza virus are activated during primary HIV infection. J. Immunol. *173*, 2410–2418.

Ehl, S., Hombach, J., Aichele, P., Hengartner, H., and Zinkernagel, R.M. (1997). Bystander activation of cytotoxic T cells: Studies on the mechanism and evaluation of in vivo significance in a transgenic mouse model. J. Exp. Med. *185*, 1241–1251.

Forns, X., Thimme, R., Govindarajan, S., Emerson, S.U., Purcell, R.H., Chisari, F.V., and Bukh, J. (2000). Hepatitis C virus lacking the hypervariable region 1 of the second envelope protein is infectious and causes acute resolving or persistent infection in chimpanzees. Proc. Natl. Acad. Sci. USA *97*, 13318–13323.

Fuller, M.J., and Zajac, A.J. (2003). Ablation of CD8 and CD4 T cell responses by high viral loads. J. Immunol. *170*, 477–486.

Gerdes, J., Lemke, H., Baisch, H., Wacker, H.H., Schwab, U., and Stein, H. (1984). Cell cycle analysis of a cell proliferation-associated human nuclear antigen defined by the monoclonal antibody Ki-67. J. Immunol. *133*, 1710–1715.

Grayson, J.M., Zajac, A.J., Altman, J.D., and Ahmed, R. (2000). Cutting edge: Increased expression of Bcl-2 in antigen-specific memory CD8+ T cells. J. Immunol. *164*, 3950–3954.

Hamann, D., Baars, P.A., Rep, M.H., Hooibrink, B., Kerkhof-Garde, S.R., Klein, M.R., and van Lier, R.A. (1997). Phenotypic and functional separation of memory and effector human CD8+ T cells. J. Exp. Med. *186*, 1407–1418.

Hammarlund, E., Lewis, M.W., Hansen, S.G., Strelow, L.I., Nelson, J.A., Sexton, G.J., Hanifin, J.M., and Slifka, M.K. (2003). Duration of antiviral immunity after smallpox vaccination. Nat. Med. *9*, 1131–1137.

Harrington, L.E., van der Most, R.G., Whitton, J.L., and Ahmed, R. (2002). Recombinant vaccinia virus-induced T-cell immunity: Quantitation of the response to the virus vector and the foreign epitope. J. Virol. *76*, 3329–3337.

Hockenbery, D., Nunez, G., Milliman, C., Schreiber, R.D., and Korsmeyer, S.J. (1990). Bcl-2 is an inner mitochondrial membrane protein that blocks programmed cell death. Nature *348*, 334–336.

Hoffmeister, B., Kiecker, F., Tesfa, L., Volk, H.D., Picker, L.J., and Kern, F. (2003). Mapping T cell epitopes by flow cytometry. Methods *29*, 270–281.

Kaech, S.M., Tan, J.T., Wherry, E.J., Konieczny, B.T., Surh, C.D., and Ahmed, R. (2003). Selective expression of the interleukin 7 receptor identifies effector CD8 T cells that give rise to long-lived memory cells. Nat. Immunol. *4*, 1191–1198.

Ku, C.C., Murakami, M., Sakamoto, A., Kappler, J., and Marrack, P. (2000). Control of homeostasis of CD8+ memory T cells by opposing cytokines. Science *288*, 675–678.

Lau, L.L., Jamieson, B.D., Somasundaram, T., and Ahmed, R. (1994). Cytotoxic T-cell memory without antigen. Nature *369*, 648–652.

Lauer, G.M., Ouchi, K., Chung, R.T., Nguyen, T.N., Day, C.L., Purkis, D.R., Reiser, M., Kim, A.Y., Lucas, M., Klenerman, P., and Walker, B.D. (2002). Comprehensive analysis of CD8(+)-T-cell responses against hepatitis C virus reveals multiple unpredicted specificities. J. Virol. *76*, 6104–6113.

Lechner, F., Wong, D.K., Dunbar, P.R., Chapman, R., Chung, R.T., Dohrenwend, P., Robbins, G., Phillips, R., Klenerman, P., and Walker, B.D. (2000). Analysis of successful immune responses in persons infected with hepatitis C virus. J. Exp. Med. *191*, 1499–1512.

Littaua, R.A., Takeda, A., Cruz, J., and Ennis, F.A. (1992). Vaccinia virus-specific human CD4+ cytotoxic T-lymphocyte clones. J. Virol. *66*, 2274–2280.

Lukacher, A.E., Moser, J.M., Hadley, A., and Altman, J.D. (1999). Visualization of polyoma virus-specific CD8+ T cells in vivo during infection and tumor rejection. J. Immunol. *163*, 3369–3378.

McCarthy, K., Downie, A.W., and Bradley, W.H. (1958). The antibody response in man following infection with viruses of the pox group. II. Antibody response following vaccination. J. Hyg. (Lond.) *56*, 466–478.

McMichael, A.J., and Rowland-Jones, S.L. (2001). Cellular immune responses to HIV. Nature *410*, 980–987.

McNally, J.M., and Welsh, R.M. (2002). Bystander T cell activation and attrition. Curr. Top. Microbiol. Immunol. *263*, 29–41.

Miller, J.D., Weber, D.A., Ibegbu, C., Pohl, J., Altman, J.D., and Jensen, P.E. (2003). Analysis of HLA-E peptide-binding specificity and contact residues in bound peptide required for recognition by CD94/NKG2. J. Immunol. *171*, 1369–1375.

Moss, B. (1999). Vaccines, Third Edition (Philadelphia: W.B. Saunders Company).

Murali-Krishna, K., Altman, J.D., Suresh, M., Sourdive, D.J., Zajac, A.J., Miller, J.D., Slansky, J., and Ahmed, R. (1998). Counting antigen-specific CD8 T cells: A reevaluation of bystander activation during viral infection. Immunity *8*, 177–187.

Murali-Krishna, K., Lau, L.L., Sambhara, S., Lemonnier, F., Altman, J., and Ahmed, R. (1999). Persistence of memory CD8 T cells in MHC class I-deficient mice. Science *286*, 1377–1381.

Newman, F.K., Frey, S.E., Blevins, T.P., Mandava, M., Bonifacio, A., Jr., Yan, L., and Belshe, R.B. (2003). Improved assay to detect neutralizing antibody following vaccination with diluted or undiluted vaccinia (Dryvax) vaccine. J. Clin. Microbiol. *41*, 3154–3157.

Pitcher, C.J., Hagen, S.I., Walker, J.M., Lum, R., Mitchell, B.L., Maino, V.C., Axthelm, M.K., and Picker, L.J. (2002). Development and homeostasis of T cell memory in rhesus macaque. J. Immunol. *168*, 29–43.

Poland, J.D., Calisher, C.H., Monath, T.P., Downs, W.G., and Murphy, K. (1981). Persistence of neutralizing antibody 30–35 years after immunization with 17D yellow fever vaccine. Bull. World Health Organ. *59*, 895–900.

Precopio, M.L., Betts, M.R., Parrino, J., Price, D.A., Gostick, E., Ambrozak, D.R., Asher, T.E., Douek, D.C., Harari, A., Pantaleo, G., et al. (2007). Immunization with vaccinia virus induces polyfunctional and phenotypically distinctive CD8(+) T cell responses. J. Exp. Med. *204*, 1405–1416.

Reinhardt, B., Jaspert, R., Niedrig, M., Kostner, C., and L'Age-Stehr, J. (1998). Development of viremia and humoral and cellular parameters of immune activation after vaccination with yellow fever virus strain 17D: A model of human flavivirus infection. J. Med. Virol. *56*, 159–167.

Rice, C.M., Grakoui, A., Galler, R., and Chambers, T.J. (1989). Transcription of infectious yellow fever RNA from full-length cDNA templates produced by in vitro ligation. New Biol. *1*, 285–296.

Rock, M.T., Yoder, S.M., Wright, P.F., Talbot, T.R., Edwards, K.M., and Crowe, J.E., Jr. (2005). Differential regulation of granzyme and perforin in effector and memory T cells following smallpox immunization. J. Immunol. *174*, 3757–3764.

Rock, M.T., Yoder, S.M., Talbot, T.R., Edwards, K.M., and Crowe, J.E., Jr. (2006). Cellular immune responses to diluted and undiluted aventis pasteur smallpox vaccine. J. Infect. Dis. *194*, 435–443.

Roos, M.T., van Lier, R.A., Hamann, D., Knol, G.J., Verhoofstad, I., van Baarle, D., Miedema, F., and Schellekens, P.T. (2000). Changes in the composition of circulating CD8+ T cell subsets during acute epstein-barr and human immunodeficiency virus infections in humans. J. Infect. Dis. *182*, 451–458.

Sakai, A., Takikawa, S., Thimme, R., Meunier, J.C., Spangenberg, H.C., Govindarajan, S., Farci, P., Emerson, S.U., Chisari, F.V., Purcell, R.H., and Bukh, J. (2007). In vivo study of the HC-TN strain of hepatitis C virus recovered from a patient with fulminant hepatitis: RNA transcripts of a molecular clone (pHC-TN) are infectious in chimpanzees but not in Huh7.5 cells. J. Virol. *81*, 7208–7219.

Sallusto, F., Lenig, D., Forster, R., Lipp, M., and Lanzavecchia, A. (1999). Two subsets of memory T lymphocytes with distinct homing potentials and effector functions. Nature *401*, 708–712.

Schluns, K.S., Kieper, W.C., Jameson, S.C., and Lefrancois, L. (2000). Interleukin-7 mediates the homeostasis of naive and memory CD8 T cells in vivo. Nat. Immunol. *1*, 426–432.

Slifka, M.K., Rodriguez, F., and Whitton, J.L. (1999). Rapid on/off cycling of cytokine production by virus-specific CD8+ T cells. Nature *401*, 76–79.

Tan, J.T., Ernst, B., Kieper, W.C., LeRoy, E., Sprent, J., and Surh, C.D. (2002). Interleukin (IL)-15 and IL-7 jointly regulate homeostatic proliferation of memory phenotype CD8+ cells but are not required for memory phenotype CD4+ cells. J. Exp. Med. *195*, 1523–1532.

Tan, L.C., Gudgeon, N., Annels, N.E., Hansasuta, P., O'Callaghan, C.A., Rowland-Jones, S., McMichael, A.J., Rickinson, A.B., and Callan, M.F. (1999). A re-evaluation of the frequency of CD8+ T cells specific for EBV in healthy virus carriers. J. Immunol. *162*, 1827–1835.

Terajima, M., Cruz, J., Raines, G., Kilpatrick, E.D., Kennedy, J.S., Rothman, A.L., and Ennis, F.A. (2003). Quantitation of CD8+ T cell responses to newly identified HLA-A*0201-restricted T cell epitopes conserved among vaccinia and variola (smallpox) viruses. J. Exp. Med. *197*, 927–932.

Thimme, R., Bukh, J., Spangenberg, H.C., Wieland, S., Pemberton, J., Steiger, C., Govindarajan, S., Purcell, R.H., and Chisari, F.V. (2002). Viral and immunological determinants of hepatitis C virus clearance, persistence, and disease. Proc. Natl. Acad. Sci. USA *99*, 15661–15668.

Thimme, R., Wieland, S., Steiger, C., Ghrayeb, J., Reimann, K.A., Purcell, R.H., and Chisari, F.V. (2003). CD8(+) T cells mediate viral clearance and disease pathogenesis during acute hepatitis B virus infection. J. Virol. *77*, 68–76.

Tomiyama, H., Takata, H., Matsuda, T., and Takiguchi, M. (2004). Phenotypic classification of human CD8+ T cells reflecting their function: Inverse correlation between quantitative expression of CD27 and cytotoxic effector function. Eur. J. Immunol. *34*, 999–1010.

Tough, D.F., Borrow, P., and Sprent, J. (1996). Induction of bystander T cell proliferation by viruses and type I interferon in vivo. Science *272*, 1947–1950.

Tough, D.F., and Sprent, J. (1998). Bystander stimulation of T cells in vivo by cytokines. Vet. Immunol. Immunopathol. *63*, 123–129.

Tuuminen, T., Kekalainen, E., Makela, S., Ala-Houhala, I., Ennis, F.A., Hedman, K., Mustonen, J., Vaheri, A., and Arstila, T.P. (2007). Human CD8+ T cell memory generation in Puumala hantavirus infection occurs after the acute phase and is associated with boosting of EBV-specific CD8+ memory T cells. J. Immunol. *179*, 1988–1995.

Urbani, S., Boni, C., Missale, G., Elia, G., Cavallo, C., Massari, M., Raimondo, G., and Ferrari, C. (2002). Virus-specific CD8+ lymphocytes share the same effector-memory phenotype but exhibit functional differences in acute hepatitis B and C. J. Virol. *76*, 12423–12434.

van der Most, R.G., Murali-Krishna, K., Lanier, J.G., Wherry, E.J., Puglielli, M.T., Blattman, J.N., Sette, A., and Ahmed, R. (2003). Changing immunodominance patterns in antiviral CD8 T-cell responses after loss of epitope presentation or chronic antigenic stimulation. Virology *315*, 93–102.

van Leeuwen, E.M., Gamadia, L.E., Baars, P.A., Remmerswaal, E.B., ten Berge, I.J., and van Lier, R.A. (2002). Proliferation requirements of cytomegalovirus-specific, effector-type human CD8+ T cells. J. Immunol. *169*, 5838–5843.

Vranjkovic, A., Crawley, A.M., Gee, K., Kumar, A., and Angel, J.B. (2007). IL-7 decreases IL-7 receptor alpha (CD127) expression and induces the shedding of CD127 by human CD8+ T cells. Int. Immunol. *19*, 1329–1339.

Wherry, E.J., Becker, T.C., Boone, D., Kaja, M.K., Ma, A., and Ahmed, R. (2002). Homeostatic proliferation but not the generation of virus specific memory CD8 T cells is impaired in the absence of IL-15 or IL-15Ralpha. Adv. Exp. Med. Biol. *512*, 165–175.

Wherry, E.J., Blattman, J.N., Murali-Krishna, K., van der Most, R., and Ahmed, R. (2003a). Viral persistence alters CD8 T-cell immunodominance and tissue distribution and results in distinct stages of functional impairment. J. Virol. *77*, 4911–4927.

Wherry, E.J., Teichgräber, V., Becker, T.C., Masopust, D., Kaech, S.M., Antia, R., von Andrian, U.H., and Ahmed, R. (2003b). Lineage relationship and protective immunity of memory CD8 T cell subsets. Nat. Immunol. *4*, 225–234.

Wherry, E.J., Barber, D.L., Kaech, S.M., Blattman, J.N., and Ahmed, R. (2004). Antigen-independent memory CD8 T cells do not develop during chronic viral infection. Proc. Natl. Acad. Sci. USA *101*, 16004–16009.

Wyeth (2002). Package Insert: Dryvax (Smallpox Vaccine, Dried, Calf Lymph Type). (US Food and Drug Administration [CBER]), pp. 1–8.

Zajac, A.J., Blattman, J.N., Murali-Krishna, K., Sourdive, D.J., Suresh, M., Altman, J.D., and Ahmed, R. (1998). Viral immune evasion due to persistence of activated T cells without effector function. J. Exp. Med. *188*, 2205–2213.

Zarozinski, C.C., and Welsh, R.M. (1997). Minimal bystander activation of CD8 T cells during the virus-induced polyclonal T cell response. J. Exp. Med. *185*, 1629–1639.